

Title	Alignment of Grain Boundary in a Si film Crystallized by a Linearly Polarized Laser Beam on a Glass Substrate
Author(s)	Horita, S; Nakata, Y; Shimoyama, A
Citation	Applied Physics Letters, 78(15): 2250-2252
Issue Date	2001-04
Type	Journal Article
Text version	publisher
URL	<a href="http://hdl.handle.net/10119/3377">http://hdl.handle.net/10119/3377</a>
Rights	Copyright 2001 American Institute of Physics. This article may be downloaded for personal use only. Any other use requires prior permission of the author and the American Institute of Physics. The following article appeared in Susumu Horita, Y. Nakata, and A. Shimoyama, Applied Physics Letters 78(15), 2250-2252 (2001) and may be found at <a href="http://link.aip.org/link/?apl/78/2250">http://link.aip.org/link/?apl/78/2250</a> .
Description	

## Alignment of grain boundary in a Si film crystallized by a linearly polarized laser beam on a glass substrate

Susumu Horita,<sup>a)</sup> Y. Nakata, and A. Shimoyama

*School of Materials Science, Japan Advanced Institute of Science and Technology, Hokuriku, Tatsunokuchi, Ishikawa 923-1292, Japan*

(Received 10 July 2000; accepted for publication 13 February 2001)

We performed crystallization of an amorphous Si film deposited on a Pyrex glass substrate using a Nd:YAG pulse-laser beam with linear polarization. It was found that, in the crystallized film, the grain boundaries were aligned with a period of about 550 nm or the wavelength of the laser beam. Meanwhile, in the Si film crystallized by circularly polarized beam that passed through the  $\lambda/4$  plate, the grain boundaries were randomly generated. This means that linear polarization of the laser beam is essential to align grain boundaries periodically or to produce a periodic temperature distribution in the irradiated Si film. © 2001 American Institute of Physics. [DOI: 10.1063/1.1362336]

Polycrystalline silicon (poly-Si) thin films fabricated on glass substrates at low temperature less than 600 °C are greatly useful in microelectronics industry since they are currently applied to thin film transistors (TFTs) for liquid crystal display. They also have potential to apply to LSI circuits in the future. Among several fabrication methods of poly-Si thin film on a glass substrate, pulse-laser annealing (PLA) method is effective to produce large grain with high carrier mobility.<sup>1,2</sup> PLA method is that an intense, short duration, and short wavelength light beam emitted from a pulse-laser heats an amorphous Si (*a*-Si) film deposited on the substrate to its melting point to be crystallized during the solidification process while keeping the nonheated resistant glass substrate at sufficiently low temperature. Ideal TFT requires the entire active region to be free of grain boundary because it reduces the carrier mobility, fluctuates the threshold voltage, and increases the off current of the TFT. Therefore, the location and enlargement of grain boundary should be well controlled. For that purpose, the modulated PLA methods have been proposed using absorption layer,<sup>3,4</sup> prepatterned poly-Si layer,<sup>4,5</sup> and so on.<sup>6-9</sup> Also, the interference PLA methods which produce the periodic temperature distribution have been introduced by some authors using a beam splitter<sup>10</sup> and a phase-shift mask.<sup>11</sup> They can artificially control the temperature distribution in the Si film so as to reduce the random nucleation and unify the solidification direction of the molten Si.

On the other hand, it has been reported that linearly polarized laser irradiation induces spatially periodic structures on the surfaces of semiconductor,<sup>12-15</sup> metal,<sup>14,16</sup> and polymers.<sup>17</sup> This means that the laser irradiation produces a periodic temperature distribution on the surface. For most of the case, the periodic spacing of the surface structure is formulated from Rayleigh's diffraction conditions as  $\lambda/[n_0(1 \pm \sin \theta_i)]$  for a *p*-polarized beam, where  $\lambda$  is the incident laser wavelength,  $\theta_i$  is the angle from the normal incident, and  $n_0$  is the refractive index of the incident medium above the surface. The periodic pattern has alternating peaks and valleys forming parallel lines. The direction of the stripe is

perpendicular to the electric field vector of the incident beam. By using this phenomenon, it can be expected that the grain boundary location in the PLA crystallized Si film is controlled without additional processes of depositing and/or patterning and additional optical components that the aforementioned PLA methods need. Therefore, we tried the PLA crystallization of an *a*-Si film deposited on a glass substrate by using a Nd:YAG pulse-laser beam with linear polarization. In this letter, the experimental results are described and briefly discussed.

In order to check the irradiation condition, a Si substrate was used as a sample and the irradiated surface was observed by atomic force microscopy (AFM). In this case, the number of the irradiation pulse was 6000. For crystallization, a 60 nm thick *a*-Si film was deposited on a Pyrex glass substrate at 350 °C and was irradiated by a Nd:YAG pulse-laser beam with  $\theta_i=1.8^\circ$  at the same temperature in the ultrahigh vacuum chamber. The wavelength, the repetition frequency, and the pulse width of the laser beam were 532 nm, 10 Hz, and 6-7 ns, respectively. The total beam power was 1 W, the beam diameter was about 10 mm, and the number of the irradiation laser pulse was 3 to 5. After crystallization, in order to reveal the grain boundary of the sample, Secco etching<sup>18</sup> was performed and the surface was characterized by scanning electron microscope (SEM) and the Nomarski optical microscope. The degree of crystallization of some samples was estimated by Raman spectroscopy.

Figure 1(a) shows the AFM image and the surface periodic profile of the (100) Si substrate irradiated by the linearly polarized Nd:YAG pulse laser. In this case, the substrate temperature was 220 °C and the laser fluence was 200 mJ/cm<sup>2</sup>. We can recognize from Fig. 1 that the periodic line stripes perpendicular to the electric field are regularly produced with the period of about 550 nm or  $\lambda/(1 + \sin 1.8^\circ)$  on the surface. Also, from the surface profile of the inset, the height between the peak and valley is  $23 \pm 1$  nm. It can be considered that the ripple is formed due to the expansion and the shrinkage of Si during the melting and solidification on the substrate. So, we can say that linearly polarized laser beam generates the periodic temperature distribution on the Si substrate.

<sup>a)</sup>Electronic mail: horita@jaist.ac.jp

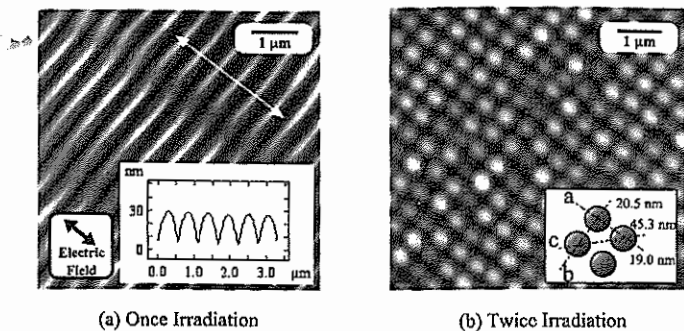


FIG. 1. AFM images of the periodic surface structure of the Si substrates. (a) The substrate was irradiated once and the inset is its surface profile along the white arrow in the image. (b) The substrate was irradiated twice. After the first irradiation, the substrate was rotated by  $90^\circ$  to perform the second irradiation. The inset is a schematic drawing of the island surface structure.

However, we hardly observed the visible ripple until the pulse number was less than 2000. This is because the fluence is subthreshold or lower than the single-pulse threshold at which the ripple is formed by one shot. It has been clearly demonstrated that the number of shots required to produce a ripple pattern increased rapidly as the pulse energy is reduced below the single-shot threshold level.<sup>19</sup>

Figure 1(b) shows the AFM image and its schematic drawing of the Si surface irradiated twice, where the second irradiation was performed after the first-irradiated Si substrate was rotated by  $90^\circ$ . It can be seen from Fig. 1(b) that many spherical islands were aligned orderly with the period of about 550 nm in two dimension. These periodically aligned islands are produced by separating the stripes due to the first irradiation with the second irradiation. In the inset of Fig. 1(b), the numbers indicate the heights of some islands along each broken line. The lines a and b are parallel to the stripes produced by the first and the second irradiation, respectively. It can be seen that the height of the island along the line c is 45 nm which is roughly equal to the sum of the heights along the lines a and b. This is because the valley region under the line c intersects with lines a and b and were irradiated twice independently. However, as can be seen, the height of line a is slightly different from line b, and they are different from  $23 \pm 1$  nm of Fig. 1(a), too. This is because the laser power density is not always uniform in the scale of  $\mu\text{m}$  or sub- $\mu\text{m}$  order. In fact, due to this nonuniformity of the laser power density, the distortion of the ripple line occurs like Fig. 1(a), the sizes of spherical island are different like Fig. 1(b), and the measurement difference in height was less than  $\pm 3$  nm.

Figures 2(a) and 2(b) show the SEM images of the Si films Secco etched after crystallization. In the case of Fig. 2(b), the laser beam passed through the  $\lambda/4$  plate before irradiating the film. The fluences in Figs. 2(a) and 2(b) were  $220 \text{ mJ/cm}^2$ . It can be seen from Fig. 2(a) that the grain boundaries are aligned with the period of about 550 nm. This means that the grain boundary location is controlled by the periodic temperature distribution produced by the linearly polarized pulse-laser irradiation in the Si film. Nucleation occurs close to the linear region of the minimal temperature in each periodic stripe while the rest is molten. As the molten Si film cools, the solidification fronts progress from the linear nucleation region to both sides of the maximal tempera-

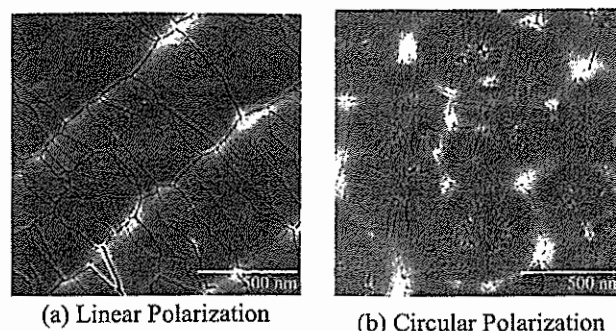


FIG. 2. Scanning electron microscopy images of the Secco etched Si films crystallized by (a) linearly polarized and (b) circularly polarized laser beams. In the case of (b), the laser beam passed through the  $\lambda/4$  plate.

ture regions where two fronts collide with each other and, as a result, the linear grain boundaries are formed periodically. However, it is observed that there are many short grain boundaries almost normal to the periodic grain boundaries. It can be considered that these short grain boundaries were generated by the turbulence of the temperature distribution due to the nonuniformity of the laser power density. If the random nucleation can be reduced by improving the uniformity and the stability of the beam power density, the generation of the disordered grain boundary may be suppressed. In contrast with the aligned grain boundary, from Fig. 2(b), we observe that all the grain boundaries in the crystallized Si film are randomly generated. This is because the linear polarization of the Nd:YAG laser beam was changed to the circular one by passing through the  $\lambda/4$  plate. So, we conclude that linear polarization is an essential factor to form the periodic thermal distribution in the Si film on the Pyrex glass substrate.

On the other hand, by Raman spectroscopy measurement, we observed that the film was crystallized at the fluence more than  $120 \text{ mJ/cm}^2$ . The fluences from  $120$  to  $220 \text{ mJ/cm}^2$  are not much different from those of the excimer-laser crystallization method, in general. For example, it has been reported that the threshold and optimum fluences for crystallization were  $155$  and  $262 \text{ mJ/cm}^2$ , respectively, for the  $50 \text{ nm}$  thickness  $a\text{-Si}$  film on a fused quartz substrate at room temperature by KrF excimer laser ( $248 \text{ nm}$ ) with the pulse width of  $25 \text{ ns}$ .<sup>20</sup> In our case, the optimum fluence has not been determined yet. The small difference in fluence between the two cases seems to be strange because the absorption coefficient  $\alpha$  for  $248 \text{ nm}$  is  $1.4 \times 10^6 \text{ 1/cm}$  and is much larger than  $2.0 \times 10^5 \text{ 1/cm}$  for  $532 \text{ nm}$ .<sup>21</sup> However, the absorptances of the  $60 \text{ nm}$  thick  $a\text{-Si}$  film/Pyrex glass substrate structure for  $248$  and  $532 \text{ nm}$  are calculated to be about  $42\%$  and  $50\%$ , respectively, considering the multireflection in the film. So, we can say that a primary reason of the small difference in fluence is rough equality in absorptance between the two cases. Also, this rough equality in absorptance can be explained as follows. Because the intensity reflectances of  $a\text{-Si}$  for  $248$  and  $532 \text{ nm}$  are  $0.55$  and  $0.41$ ,<sup>21</sup> respectively, the beam energies traversing the film surface are almost same for the two wavelengths. Further, the absorption length  $1/\alpha$  for  $532 \text{ nm}$  is about  $50 \text{ nm}$  and is a little shorter than the film thickness so that most of the beam energy traversing the film surface is absorbed in the film. Since the threshold and optimum flu-

ences for crystallization depend on other parameters such as pulse width, substrate temperature, absorption coefficient, film thickness, and so on, the strict reason of the small difference in fluence may be more complicated. After etching the crystallized Si film, it was observed by the Nomarski optical microscope that the surface of the Pyrex glass was fairly smooth without reaction product with Si. Therefore, it can be considered that, during the melting of the Si film, the temperature of the substrate surface was effectively low enough to reduce the chemical reaction between the molten Si and the substrate and to keep the substrate surface flat.

We demonstrated that in the Si film crystallized by the linearly polarized PLA method, the grain boundaries were aligned with the period of about  $\lambda/(1 + \sin 1.8^\circ)$  on the Pyrex glass substrate. Therefore, it can be said that this method is useful to control the grain boundary location without additional process and optical components.

<sup>1</sup>T. Sameshima, S. Usui, and M. Sekiya, *IEEE Electron Device Lett.* **7**, 276 (1986).

<sup>2</sup>K. Sera, F. Okumura, H. Uchida, S. Itoh, S. Kaneko, and K. Hotta, *IEEE Electron Device Lett.* **36**, 2868 (1989).

<sup>3</sup>H. J. Kim and J. S. Im, *Appl. Phys. Lett.* **68**, 1513 (1996).

<sup>4</sup>M. Ozawa, C.-H. Oh, and M. Matsumura, *Jpn. J. Appl. Phys., Part 1* **38**, 5700 (1999).

<sup>5</sup>A. Hara and N. Sasaki, *Jpn. J. Appl. Phys., Part 2* **39**, L1 (2000).

<sup>6</sup>D.-H. Choi, K. Shimizu, O. Sugiura, and M. Matsumura, *Jpn. J. Appl. Phys., Part 1* **31**, 4545 (1992).

<sup>7</sup>K. Shimizu, O. Sugiura, and M. Matsumura, *IEEE Electron Device Lett.* **40**, 112 (1993).

<sup>8</sup>R. Ishihara and P. C. van der Wilt, *Jpn. J. Appl. Phys., Part 2* **37**, L15 (1998).

<sup>9</sup>L. Mariucci, R. Carluccio, A. Pecora, V. Foglietti, G. Fortunato, and D. D. Sala, *Jpn. J. Appl. Phys., Part 2* **38**, L907 (1999).

<sup>10</sup>B. Rezek, C. E. Nebel, and M. Stutzmann, *Jpn. J. Appl. Phys., Part 2* **38**, L1083 (1999).

<sup>11</sup>C. H. Oh, M. Ozawa, and M. Matsumura, *Jpn. J. Appl. Phys., Part 2* **37**, L492 (1998).

<sup>12</sup>M. Oron and G. Sørensen, *Appl. Phys. Lett.* **35**, 782 (1979).

<sup>13</sup>J. F. Young, J. E. Sipe, J. S. Preston, and H. M. van Driel, *Appl. Phys. Lett.* **41**, 261 (1982).

<sup>14</sup>J. F. Young, J. S. Preston, H. M. van Driel, and J. E. Sipe, *Phys. Rev. B* **27**, 1155 (1983).

<sup>15</sup>A. E. Siegman and P. M. Fauchet, *IEEE J. Quantum Electron.* **22**, 1384 (1986).

<sup>16</sup>Y. Kawakami, E. Ozawa, and S. Sasaki, *Appl. Phys. Lett.* **74**, 3954 (1999).

<sup>17</sup>P. E. Dyer and R. J. Farley, *Appl. Phys. Lett.* **57**, 765 (1990).

<sup>18</sup>F. Secco d'Aragano, *J. Electrochem. Soc.* **119**, 948 (1972).

<sup>19</sup>P. M. Fauchet, *Phys. Lett. A* **93**, 155 (1983).

<sup>20</sup>M. Hatano, S. Moon, and M. Lee, *J. Appl. Phys.* **87**, 36 (2000).

<sup>21</sup>H. Piller, in *Handbook of Optical Constants of Solids*, edited by E. D. Palik (Academic, San Diego, 1985), p. 571.